Absolute Cross Sections and Angular Distributions for Charged Particles from Lithium-Lithium Nuclear Reactions*

M. N. HUBERMAN, M. KAMEGAI, AND G. C. MORRISON
Enrico Fermi Institute for Nuclear Studies, University of Chicago, Chicago, Illinois
(Received 22 August 1962)

Angular distributions in the barycentric coordinate system are presented for 24 charged-particle emissions from Li^7Li^7, Li^7Li^6, and Li^6Li^6 interactions. These have been integrated, and the resulting total cross sections are tabulated. The total cross-section sums for a given projectile target combination are in reasonable agreement with theoretical estimates based on barrier penetration with nuclear radii given by $r_0A^{1/3}$ with $r_0=1.5$ F. The largest total cross sections measured are approximately 40×10^{-28} cm^2. The angular distributions from Li^6Li^6 and Li^7Li^7 are symmetrical about 90° by necessity, those from Li^7Li^6 are, in general, asymmetric and difficult to reconcile with a simple compound-nucleus interpretation of the reactions. Most of the intense particle emissions are cases in which the residual nucleus can be formed by Li^7 capturing a deuteron or an alpha from Li^6, or by Li^6 capturing an alpha from Li^7. To produce high cross sections these captures must be with $l=0$ between the reacting clusters. The evidence supports the hypothesis that a prominent but not necessarily exclusive reaction mechanism is for one of the Li-Li reacting partners to be distorted into "reacting clusters," consisting of an α cluster from either of the lithiums, and a deuteron cluster from Li^6 or a triton cluster from Li^7.

INTRODUCTION

FOR several years we have been engaged in a study of the charged particles produced when 2-MeV Li ions bombard lithium targets. Separated isotopes of lithium were used for the projectile beam and the targets, and the protons, deuterons, tritons, and alpha particles from the resultant Li-Li nuclear reactions were distinguished and counted in a particle selector system.

In the earlier stages of this work, only relative values of $d\sigma/d\Omega$ were measured at various angles to the beam. Certain interesting results appeared in a few of these relative measurements and have been reported in preliminary communications.[1-3] The results have since then been extended to a total of 38 charged-particle groups and the absolute cross sections have been determined. During this period studies of the Li-Li reactions have appeared by various authors.[4-6] The investigations of McGrath, and of Berkowitz *et al.*, are particularly pertinent to the present work, as they have, from a survey of the emitted gamma rays, made an estimate of the relative probabilities of production of various gamma-ray emitters, i.e., of excited states of the nuclear products. In order to reduce their measured relative gamma-ray intensities to populations of states, they have used our results on the groups of particles from $Li^7(Li^7,t)B^{11}$, $Li^7(Li^6,d)B^{11}$, and $Li^6(Li^6,p)B^{11}$. Thus, their work is not completely independent, but it covers a considerable number of reactions not observed by us, either because charged particles were not produced (i.e., neutron producing reaction) or the charged particles were of energies and types not separable by our selector system. Our results are compared with theirs in a subsequent section of this report.

Since either lithium isotope may be used as projectile or target, unless a uniform convention is followed in writing out reactions it is not clear which was which. We always give the target nucleus first, outside the parentheses; then the projectile; then the least massive of the products, and finally the heavier, residual nucleus. Thus, $Li^7(Li^6,p)B^{12}$ refers to the bombardment of a lithium-7 target with a lithium-6 beam. Arrows on the graphs showing the results of angular distributions indicate which of the isotopes, in the barycentric system, was moving in the direction specified by $\theta_c=0$.

The energies of excitation of nuclear excited states and the quantum numbers that have been assigned to them are quoted from the recently issued Landolt-Börnstein Tables.[7]

EXPERIMENTAL PROCEDURES

Lithium-ion sources such as were used in this work have been described by Allison and Kamegai.[8] The accelerator was a 2-MeV Van de Graaff of standard design. The kinetic energies used were determined by the fact that the ion beam was given a 90° deflection by an electrostatic deflector whose geometry is accurately known.[9] The charged aluminum surfaces between which the deflecting field was produced were sections of concentric spheres of radii 91.728 and 91.156 cm, the sections being those which would be formed by the spherical surfaces included between two planes parallel to a

* This work was supported in part by the United States Atomic Energy Commission.

[1] G. C. Morrison and M. N. Huberman, in *Proceedings of the Second Conference on Reactions between Complex Nuclei, Gatlinburg, Tennessee, 1960*, edited by A. Zucker, E. C. Halbert, and F. T. Howard (John Wiley & Sons, Inc., New York, 1960), p. 246.
[2] G. C. Morrison, Phys. Rev. Letters **5**, 565 (1960).
[3] G. C. Morrison, Phys. Rev. **121**, 182 (1961).
[4] E. Norbeck, Jr., Phys. **121**, 824 (1961).
[5] R. L. McGrath, Department of Physics and Astronomy, University of Iowa, Report sui-6210, 1962 (unpublished).
[6] E. Berkowitz, S. Bashkin, R. R. Carlson, S. A. Coon, and E. Norbeck, Jr., Department of Physics and Astronomy, University of Iowa, Report sui-62-8, 1962 (unpublished).
[7] H. H. Landolt and R. Börnstein, *New Series* (Springer-Verlag, Berlin, 1961), Group 1, Vol. 1.
[8] S. K. Allison and M. Kamegai, Rev. Sci. Instr. **32**, 1090 (1961).
[9] W. A. Fowler, C. C. Lauritsen, and T. Lauritsen, Rev. Sci. Instr. **18**, 818 (1947).

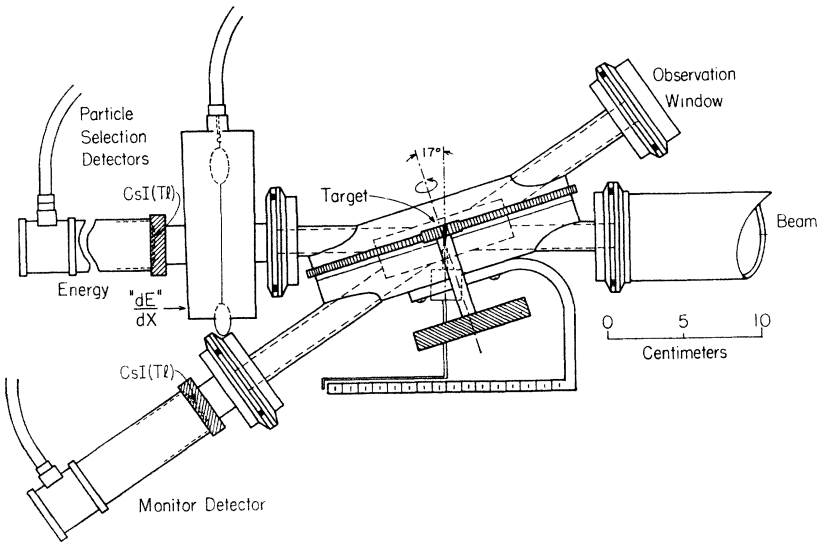

FIG. 1. Schematic drawing of the target chamber for angular distribution measurements.

diametral plane and 4.5 cm above and below it. The surface of larger radius of curvature was maintained at a positive potential by a stabilized power supply, and the inner surface was grounded. Thus, a nonrelativistic particle of positive charge $Z|e|$ which passes through the deflector along the mean radius has a kinetic energy in MeV, in a region of zero potential, equal to 80.50 $ZV|e|$, where V is the positive potential in MeV applied to the outer plate.

Since resonances do not appear in the excitation curves using lithium projectiles at less than 2.2-MeV energy, there was no necessity of defining the energy spread of the beam (by means of slits) more carefully than it was already determined by the 0.572-cm width and 143.64-cm length of the channel. This means that the beam was homogeneous in energy to 0.67%.

Although the hot filament lithium-ion source produces a remarkably "clean" lithium beam relatively free from foreign ions, the lithium beams were selected magnetically following the electrostatic deflection. The beams were deviated $22\frac{1}{2}°$ with a radius of curvature of 63.8 cm, and the Li^6 and Li^7 beams were completely separated. This provided an additional confirmation of the nature of the beam hitting a target, although material in which a high degree of separation of the lithium isotopes had already been accomplished was used in preparing the filament coatings.

For the meaurement of relative angular distributions an apparatus was constructed very similar to that described by Clarke and Paul.[10] The significant features are shown in Fig. 1 of the present report. The upper half of the cylindrical target compartment may be rotated with respect to the lower, and the axis of this rotation is inclined 17° to the horizontal plane, in which the incoming beam lies. The vacuum seal between the upper and lower halves is maintained by a large, well lubricated "O" ring. To reduce friction a ball bearing is inserted between the surfaces in relative motion during a change of angle. The two lower access tubes to the target compartment are fixed with respect to each other and to the Van de Graaff beam. One admits the beam; the other allows, in various target arrangements, reaction products or particles elastically or inelastically scattered at 17° (laboratory system) to be detected and used as a monitor.

The two access tubes to the upper compartment are fixed with respect to each other, but rotate with respect to the beam tube. One is used as an observation window to verify, by the fluorescence produced, that the beam is on the target at the desired spot. The two detectors of a particle selector system are shown attached to the other rotating arm. The angle of the upper part of the chamber with respect to the lower is read on a scale at the junction between the upper and lower halves of the target compartment; thus, the angle θ_L in the laboratory system is given in terms of the scale reading θ by

$$\sin(\tfrac{1}{2}\theta_L)=\sin(\tfrac{1}{2}\theta)\cos 17°. \quad (1)$$

Values of θ_L from 0° to 146° are mechanically possible. The lower scale of angles indicated in Fig. 1, enables a reading to be taken of the glancing angle of the beam on the plane face of the target.

The particle selection system (cf. Fig. 1) operates by the electronic analysis of two pulses from the same particle, one proportional to the specific ionization in methane, and one to the particles' total energy.[11]

The system was built and brought into successful operation by Galey and Morrison. The specific ionization ("dE/dx") signal is the pulse generated in a methane-filled cylindrical proportional counter 4.44-cm in i.d. with gas pressures in the range 2–12 cm of Hg.

[10] R. L. Clarke and E. B. Paul, Can. J. Phys. **35**, 155 (1957), cf. Fig. 2.

[11] F. A. Aschenbrenner, Phys. Rev. **98**, 657 (1955).

The particles traverse the counter at right angles to the axial collector wire. The energy (E) signal comes from absorption of the particle in a thin wafer of CsI(Tl) in optical contact with the surface of a photomultiplier tube. The two pulses cause deflection of the beam of a fast oscilloscope along the y and x axes, respectively. Illuminated spots on the scope screen characteristic of particles of the same mass but different energies lie on a set of roughly parallel curves corresponding to protons, deuterons, tritons, α particles, etc. When, for instance, α's are studied, a mask over the scope screen exposes only the α curve, which is looked at by a photomultiplier tube. A signal from this tube opens a gate allowing the E pulse to reach a 256-channel pulse-height analyzer where it is recorded in the appropriate channel.[12]

The targets for relative angular distribution measurements were made by evaporating metallic lithium onto thin aluminum foil backings. Since the targets, thus prepared, were transported in air from the evaporating vessel to the target chamber, there was undoubtedly considerable oxidation of the lithium, but conditions for correct relative $d\sigma/d\Omega$ measurements were not impaired. In a typical experiment [measurements of relative $d\sigma/d\Omega$ values for the deuteron groups from $Li^6(Li^6,d)B^{10}$] conditions were as follows. The target backing was 1.24-mg/cm^2 Al foil, the beam impinged on the surface covered with lithium, and the plane of the foil was at 45° to the beam. The deuterons entering the particle selector system passed through the Al backing. In their path to the particle selecting detector the deuterons then passed through, successively, 0.87 mg/cm^2 of Mylar plastic foil confining the gas in the proportional counter, 9.7 cm of CH_4 gas at 12.1-cm Hg pressure, and 0.16 mg/cm^2 of Al foil covering the face of the CsI(Tl) crystal. The estimated total energy loss of a 5.042-MeV nascent deuteron was 0.53 MeV. For less penetrating particles use of a 0.16 mg/cm^2 backing foil reduced the energy losses considerably. The solid angle for collection of reaction particles was 8.21×10^{-4} sr.

The protons produced from the Li-Li reactions were well suited for use for monitor counting. At 2-MeV beam energy, the proton energies from the ground states, and in the forward direction are

from $Li^7(Li^7,p)B^{13}$; $Q=$ 5.98 MeV; $E=$ 7.90 MeV.
from $Li^7(Li^6,p)B^{12}$; $Q=$ 8.34 MeV; $E=$10.28 MeV.
from $Li^6(Li^6,p)B^{11}$; $Q=$12.22 MeV; $E=$14.19 MeV.

By placing a 50 mg/cm^2 Al foil in front of the monitor detector, no charged particles except these protons can impinge on the CsI(Tl) wafer of the monitor. The normal procedure was to take the number of counts in a particle group at a given θ_L for a predetermined number of monitor counts (several thousand).

[12] A detailed account of the electronic circuits involved has been prepared by J. A. Galey and G. C. Morrison (unpublished). A limited number of copies will be distributed by the authors.

The reduction of the relative values of $d\sigma/d\Omega$ to absolute values was accomplished by measuring the absolute cross sections for the proton reactions used to produce the monitor particles. These absolute cross sections were measured at 90° to the beam, some of them with the angular distribution target chamber, and some with a special chamber, suitable only for 90° measurement, but with a larger solid angle of 3.16×10^{-3} sr.

Thick targets of LiF were prepared by evaporation of Li^6F or Li^7F, instead of the thin metallic lithium targets of the relative angular distribution measurements. Such thick targets consisted of ~0.9 mg/cm^2 LiF backed by 0.17 mg/cm^2 Al. LiF is a very stable compound whose chemical composition can safely be assumed to remain constant during vacuum evaporation. The well-known thick-target formula is

$$\frac{d\sigma}{d\Omega}=-\frac{1}{N_P N_T}\frac{dY}{dE}\frac{dE}{dx}\frac{1}{\Omega}. \tag{2}$$

N_P is the number of Li^+ ions per microcoulomb of beam. N_T is the number of Li nuclei in the target material per milligram. dY/dE is the slope of the yield curve in produced particles per microcoulomb of incident beam per MeV energy interval. dE/dx is the stopping power of the target material in MeV×cm^2/mg. Ω is the solid angle subtended by the detector.

The largest error in applying this formula may well arise in the necessity of estimating the stopping power of LiF for Li ions. Teplova *et al.*[13] found the stopping power of air for 2-MeV Li^7 ions to be 4.40 MeV/cm, and Devons and Towle[14] give 112×10^{-15} eV×cm^2/atom as the stopping power of Al for 2.74-MeV Li^7 ions. From consideration of these results, we estimate 3.0±0.2 MeV×cm^2/mg as the stopping power of LiF for 2-MeV Li^7. The value for Li^6 at the same kinetic energy lies within the uncertainty of this estimate.

In their investigations of the yield of B^{12} per μc from $Li^7(Li^6,p)B^{12}$ Norbeck and Littlejohn,[15] judging from the radioactivity of the B^{12}, found that the yield curve for the reaction apparently indicated some kind of saturation setting in above 1.8 MeV. This would be unexpected, since it requires between 4.5 and 5 MeV kinetic energy for the projectile in the laboratory system to overcome the Coulomb repulsion between two lithium nuclei, and thus we are well below the barrier. Furthermore, the excitation of a hypothetical intermediate carbon nucleus would be in the region of 28 MeV where levels of low Γ are not to be expected. In our repetition of a yield study of this reaction, counting the protons, however, we were unable to confirm this effect; (cf. Fig. 2). The yield curves continued their exponential

[13] Ia. Teplova, I. S. Dmitriev, V. S. Nikolaev, and L. N. Fateeva, Soviet Phys.—JETP **5**, 797 (1957); **15**, 31 (1962).
[14] S. Devons and J. H. Towle, Proc. Phys. Soc. (London) **A69**, 345 (1956).
[15] E. Norbeck, Jr., and C. S. Littlejohn, Phys. Rev. **108**, 754 (1957). Cf. Fig. 2.

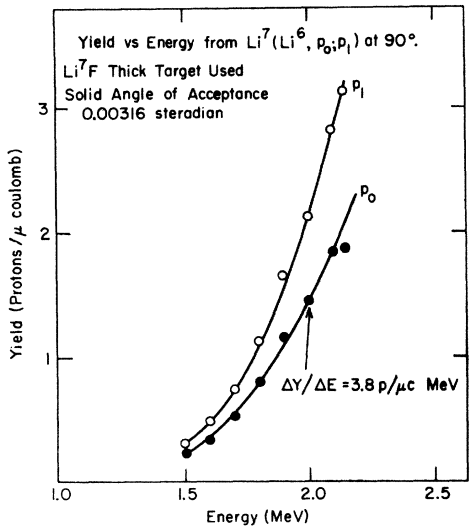

FIG. 2. Thick-target yields of protons from the Li^7Li^6 reaction when the residual B^{12} nucleus is left in the ground (p_0) state and in the first excited (p_1) state. (See Table I.) The projectile was Li^6.

rise up to 2.2 MeV. Our results gave the same order of magnitude for $d\sigma/d\Omega$ as the previous ones but larger by a factor of approximately 3. To be sure that the discrepancy was not due to the finite thickness of our "thick" targets, special targets in which LiF in bulk was melted onto a nickel button for backing were also used. These directly measured absolute values of $d\sigma/d\Omega$ are displayed (transformed to barycentric coordinates) in the graphs of the angular distributions.

The total cross sections listed in Table I, were obtained by multiplying the ordinates of the angular distributions by $\sin\theta$, integrating over angles, and multiplying by 2π. We are grateful for help from the computing group of the Argonne National Laboratory.

RESULTS

Angular Distributions

The angular distributions in the barycentric system are presented in three groups, corresponding to the Li^7Li^7, Li^7Li^6, and Li^6Li^6 reactions respectively. Figures 3 to 6 inclusive give angular distributions for proton, deuteron, triton, and α-particle groups from Li^7Li^7 bombardments at 2.1 MeV in the laboratory system. Figures 7 through 10 give distributions of products from Li^7Li^6, and Li^6Li^6 distributions appear in Figs. 11 and 12. The spread of $d\sigma/d\Omega$ values indicated by the vertical extent of the line representing an experimental datum gives the range $[d\sigma/d\Omega][1\pm m^{1/2}/m]$ where m is the number of counts recorded.

In the cases where projectile and target are identical, the drawing of curves through (and sometimes beyond) the experimental points was influenced by the fact that

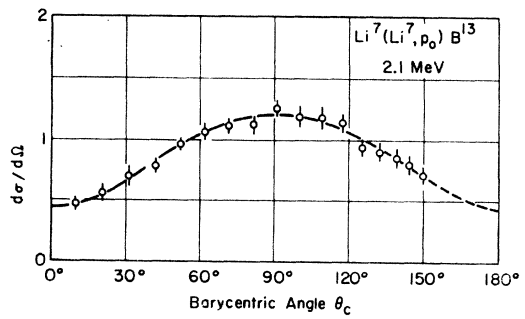

FIG. 3. Angular distribution of protons from Li^7Li^7, B^{13} being left in its ground state. For absolute values multiply ordinates by 1.25×10^{-28} cm²/sr.

TABLE I. Total cross sections at 2.1 MeV. $\sigma=2\pi\int_0^\pi(d\sigma/d\Omega)\sin\theta d\theta$.

Reaction	Q (MeV)	Excitation of residual nucleus (MeV)	J^π of residual nucleus	$\sigma(\times10^{28}$ cm²)
$Li^7(Li^7,p_0)B^{13}$	5.98	0	$3/2^-$	16
$Li^7(Li^7,p_1)B^{13}$	2.28	3.70	···	(38)
$Li^7(Li^7,p_2)B^{13}$	1.82	4.16	···	(12)
$Li^7(Li^7,p_3)B^{13}$	0.93	5.05	···	(25)
$Li^7(Li^7,p_4)B^{13}$	0.48	5.5	···	(12)
$Li^7(Li^7,d_0)B^{12}$	3.31	0	1^+	44
$Li^7(Li^7,d_1)B^{12}$	2.36	0.95	2^+, 3^+	11
$Li^7(Li^7,d_2)B^{12}$	0.69	1.67	1^-, 2^-	12
$Li^7(Li^7,t_0)B^{11}$	6.21	0	$3/2^-$	39
$Li^7(Li^7,t_1)B^{11}$	4.07	2.14	$1/2^-$	5.1
$Li^7(Li^7,t_2)B^{11}$	1.75	4.41	$5/2^-$	29
$Li^7(Li^7,t_3)B^{11}$	1.17	5.04	$3/2^-$	29
$Li^7(Li^7,\alpha_0)Be^{10}$	14.78	0	0^+	(~2)
$Li^7(Li^7,\alpha_1)Be^{10}$	11.41	3.37	2^+	29
$\alpha_2,\alpha_3,\alpha_4$	4.15–5.45	5.96–6.26	1^-, ?, ?	$\Sigma=34$
Li^7Li^6 reactions at 2.1 MeV				
$Li^7(Li^6,p_0)B^{12}$	8.34	0	1^+	3.6
$Li^7(Li^6,p_1)B^{12}$	7.39	0.95	2^+, 3^+	5.0
$Li^7(Li^6,p_2)B^{12}$	6.67	1.67	1^-, 2^-	5.3
$Li^7(Li^6,p_3)B^{12}$	5.52–5.62	2.62–2.72	···	4.0
$Li^7(Li^6,d_0)B^{11}$	7.19	0	$3/2^-$	13
$Li^7(Li^6,d_1)B^{11}$	5.05	2.14	$1/2^-$	8.9
$Li^7(Li^6,d_2)B^{11}$	2.73	4.46	$5/2^-$	9.1
$Li^7(Li^6,d_3)B^{11}$	2.15	5.04	$3/2^-$	12
$Li^7(Li^6,t_0)B^{10}$	1.99	0	3^+	7.0
$Li^7(Li^6,t_1)B^{10}$	1.27	0.72	1^+	41
$Li^7(Li^6,t_2)B^{10}$	0.25	1.74	$0^+(T=1)$	(<1)
$Li^7(Li^6,t_3)B^{10}$	−0.16	2.15	1^+	(<1)
$Li^7(Li^6,\alpha_0)Be^9$	15.22	0	$3/2^-$	6.9
Li^6Li^6 reactions at 2.1 MeV				
$Li^6(Li^6,p_0)B^{11}$	12.22	0	$3/2^-$	12
$Li^6(Li^6,p_1)B^{11}$	10.08	2.14	$1/2^-$	5.4
$Li^6(Li^6,p_2)B^{11}$	7.76	4.46	$5/2^-$	7.6
$Li^6(Li^6,p_3)B^{11}$	7.18	5.04	$3/2^-$	7.6
$Li^6(Li^6,d_0)B^{10}$	2.99	0	3^+	8.9
$Li^6(Li^6,d_1)B^{10}$	2.27	0.72	1^+	44
$Li^6(Li^6,d_2)B^{10}$	1.25	1.74	$0^+(T=1)$	<2
$Li^6(Li^6,d_3)B^{10}$	0.84	2.15	1^+	(36)
$Li^6(Li^6,\alpha_0)Be^{8a}$	21.80	0	0^+	0.56
$Li^6(Li^6,\alpha_1)Be^{8a}$	18.9	2.9	0^+, 2^+	0.54
$Li^6(Li^6,\alpha_2)Be^{8a}$	···	···	···	21

[a] These three α groups were taken at 2.0 MeV. According to M. Coste and L. Marquez (see reference 20) the particles α_2 are breakup α's from a highly excited Be^8.

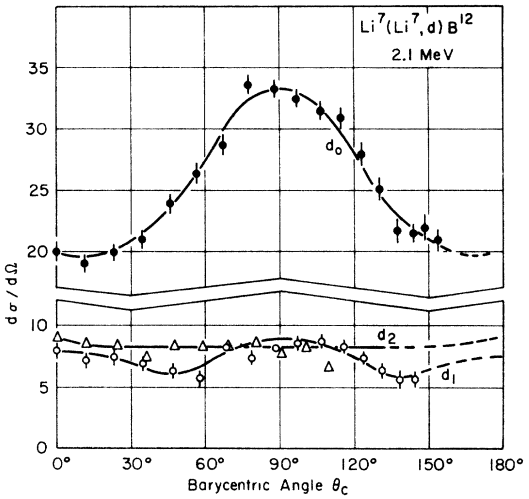

FIG. 4. Angular distributions of deuteron groups from Li^7Li^7. For absolute values multiply ordinates by 1.25×10^{-29} cm²/sr.

fore and aft asymmetry is certain, irrespective of the reaction mechanism.

In the Li^7Li^6 combinations, it was possible to follow the angular distributions from 0° to 180° in spite of the fact that the mechanical equipment could not rotate farther than 146° from the beam. To obtain the entire distribution, two different angular distributions were taken for each reaction, with target and projectile nuclei interchanged, and the bombarding energy was adjusted to compensate for the slightly different velocities of approach in the barycentric system.

Total Cross Sections

The total cross sections were obtained by integration from the absolute differential cross sections. In addition to the statistical errors in counting, they contain the errors inherent in the assignment of absolute ordinates; i.e., in the stopping power of the thick target for Li ions, the composition of the target, the solid angle of collection, and the measurement of the beam current. We

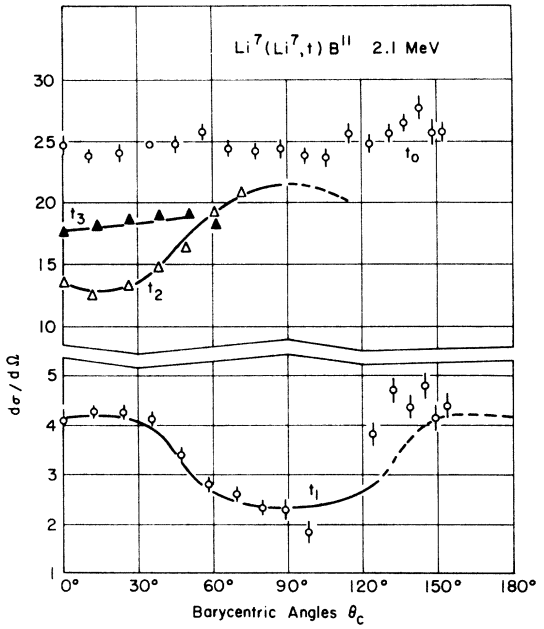

FIG. 5. Angular distributions of triton groups from Li^7Li^7. For absolute values multiply ordinates by 1.25×10^{-29} cm²/sr.

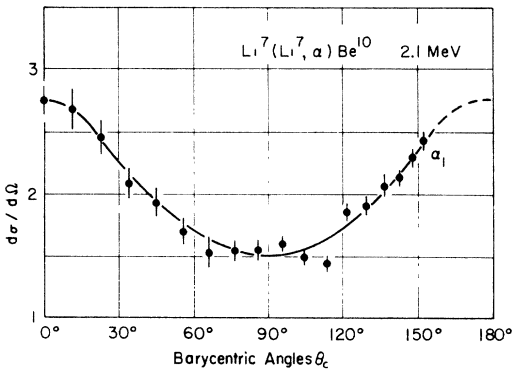

FIG. 6. Angular distribution of α's from Li^7Li^7, Be^{10} being left in its first excited (3.37 MeV) state. The α's from the ground state could be observed, but were approximately one-tenth as abundant as these. For absolute values multiply ordinates by 1.25×10^{-28} cm²/sr.

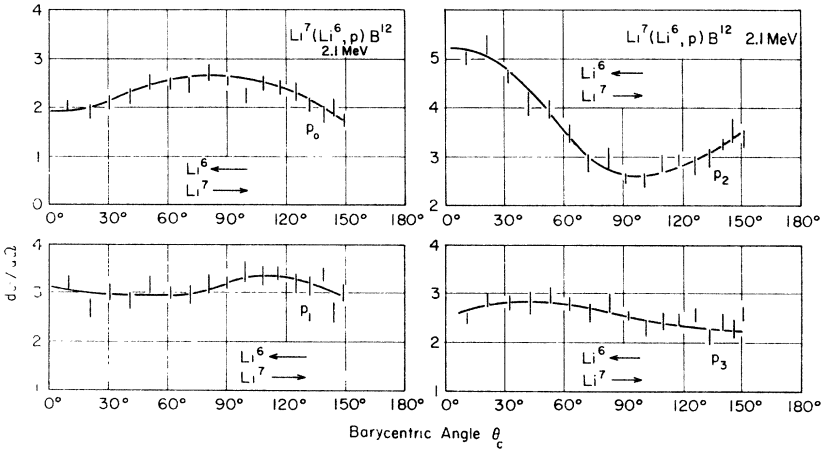

FIG. 7. Angular distributions of proton groups from Li^7Li^6. Arrows show directions of motion of the colliding nuclei in the barycentric system. For absolute values multiply ordinates by 1.25×10^{-29} cm²/sr.

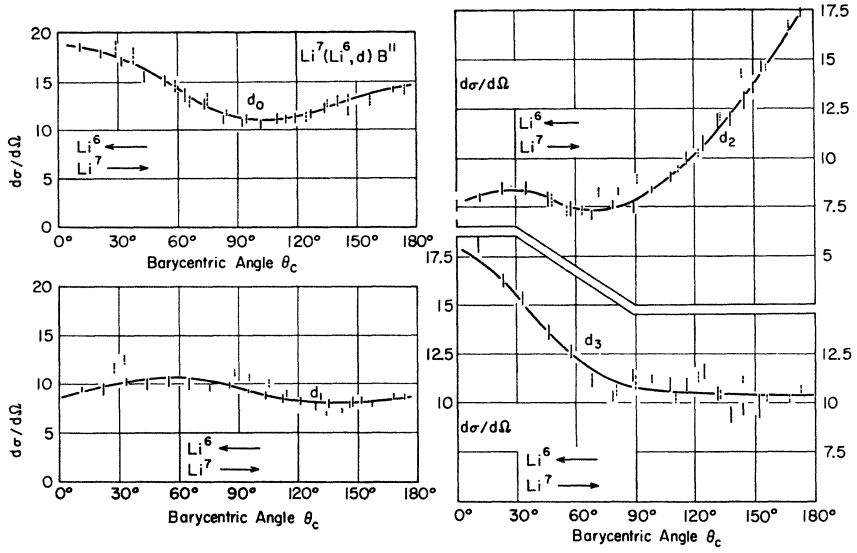

FIG. 8. Angular distributions for deuteron groups from the Li^7Li^6 reaction. Dotted points were taken with projectile and target interchanged and plotted at $(\pi-\theta_c)$. For absolute values multiply ordinates by 1.25×10^{-29} cm²/sr.

may expect errors in σ of $\pm10\%$. The results are given in Table I. In certain entries in this table, such as the proton groups arising from excited states of B^{13} in $Li^7(Li^7,p)B^{13}$, an angular distribution was not taken. The value of σ, in parenthesis, is obtained from one value of $d\sigma/d\Omega$ only, that at $\theta_c=90°$, by multiplication with 4π. This is an incorrect procedure unless the distribution should be isotropic, but from applying the same procedure to many other groups and checking with their known, correctly integrated result, it is unlikely that errors greater than $\pm25\%$ will be made by such a guess.

Figure 13 illustrates the relative total cross sections for the charged particle groups. The zero of energy in this figure represents the energy content of a hypothetical configuration in which both target and projectile have been dissociated into alpha particles and deuterons or tritons.

The energy brought into the barycentric system by the bombardment is shown by the vertical arrow extending upward from the energy level representing the undissociated target and projectile. The downward directed arrows indicate by their lengths, the kinetic energies of emitted particle groups, and by their widths, the cross sections for emission. Cross sections between

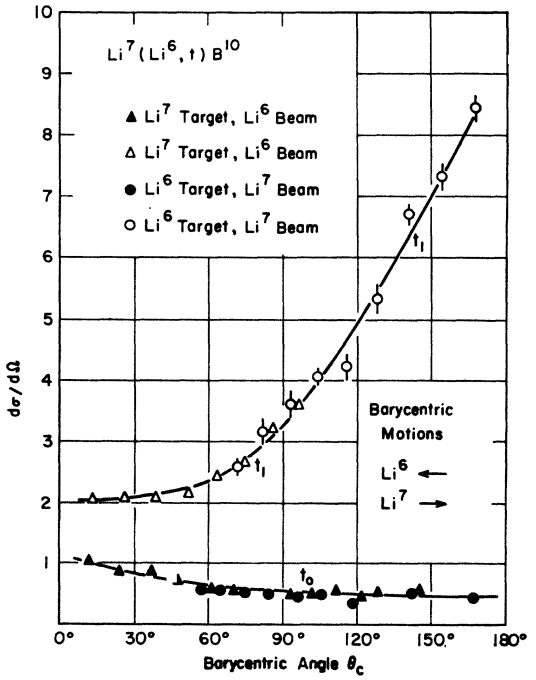

FIG. 9. Angular distributions of triton groups from Li^7Li^6. Tritons from the second and third excited states of B^{10} cannot be detected. For absolute values multiply ordinates by 1.25×10^{-28} cm²/sr.

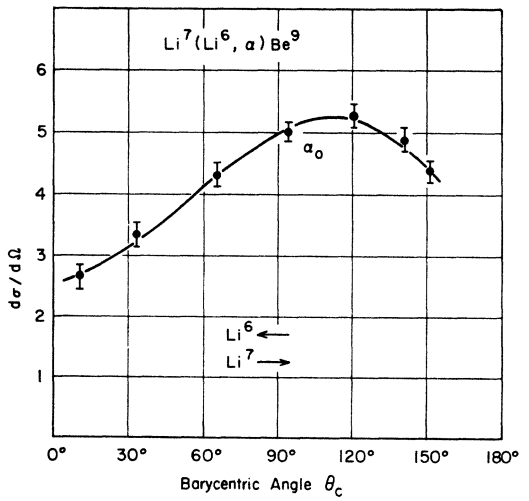

FIG. 10. Angular distribution of α's from Li^7Li^6, Be^9 being left in its ground state. For absolute values multiply ordinates by 1.25×10^{-29} cm²/sr.

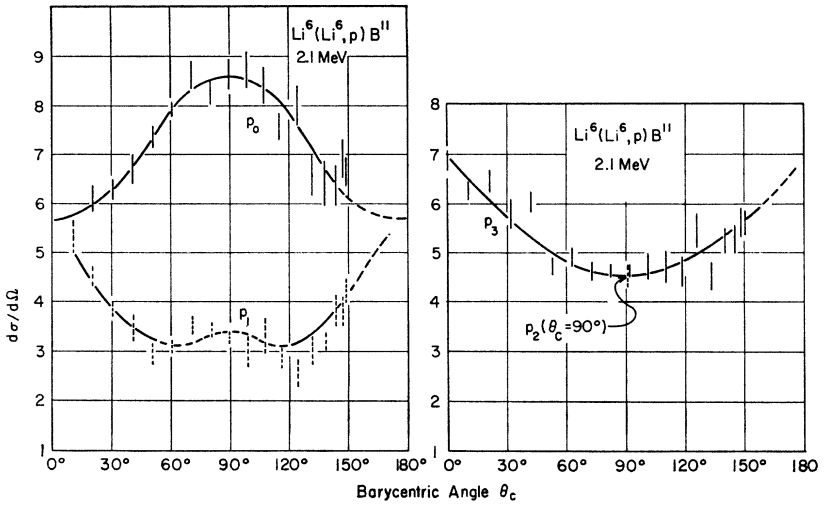

FIG. 11. Angular distributions for proton groups from Li^6Li^6. One point on the curve for the group (p_2) from the second excited state of B^{11} is shown. For absolute values multiply ordinates by 1.25×10^{-29} cm²/sr.

5 and 9×10^{-28} cm² are indicated by dashed lines; between 0 and 5×10^{-28} cm² by dotted lines.

In cases where the total cross sections have been guessed at as $4\pi[d\sigma(90°)/d\Omega]$ only the final level is indicated by a dashed arrowhead.

DISCUSSION

Total Cross Sections

At the bombarding energy of these experiments, the translational kinetic energy available in the barycentric system is well below the top of the conventional potential barrier calculated with radii given by $1.5A^{1/3}$ F. We may first investigate whether the sum of the cross sections in the exit channels for a given reaction is given, as to order of magnitude, by conventional barrier penetration calculations.

We have used the tables of Feshbach, Shapiro, and Weisskopf[16] to compute the value of

$$\sigma_c=\pi\lambda^2(2l+1)T_l, \qquad (3)$$

where σ_c may be called the cross section for barrier penetration. The theoretical values are shown in Table II, and may be compared with the experimental total cross sections of Table I. The theoretical sums in the right-hand column of Table II should, in a simple form of interpretation, give an approximate upper limit to the experimental cross-section sums. Our data on the possible exit channels from a given initial state are of course seriously limited because not all possible charged particle exit channels have been explored, and we have no information on reaction products involving the emission of neutrons. Nevertheless, the total cross-section sum for 15 exit channels from the Li^7Li^7 interaction, involving charged-particle groups arising from the ground and excited states of Be^{10}, B^{11}, B^{12}, and B^{13} is 330×10^{-28} cm² which exceeds the predicted sum by a factor of 2. In view of the sensitivity of the calculation to the assumed nuclear radius the discrepancy is not serious. The experimental sum for 13 charged-particle exit channels from Li^7Li^6 is 116×10^{-28} cm², well below the calculated 228 of Table II, and the comparison of experiment vs theory is 124×10^{-28} cm² for the sum of a few of the possible proton and deuteron groups versus 403 calculated upper limit.

This behavior is in contrast to that of the impact

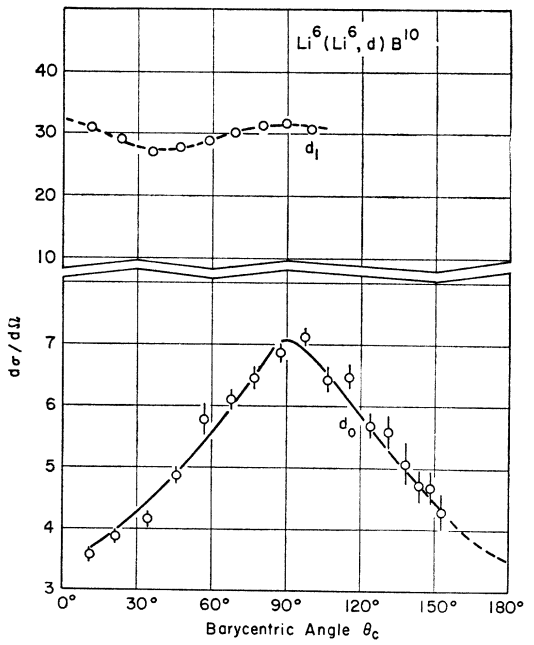

FIG. 12. Angular distributions of deuteron groups from Li^6Li^6. Deuterons from the second excited ($T=1$) state of B^{10} cannot be detected. For absolute values multiply ordinates by 1.25×10^{-29} cm²/sr.

[16] H. Feshbach, M. M. Shapiro, and V. F. Weisskopf, Nuclear Development Associates, Inc., Report NDA 15B-5, NYO 3077, White Plains, New York, (unpublished).

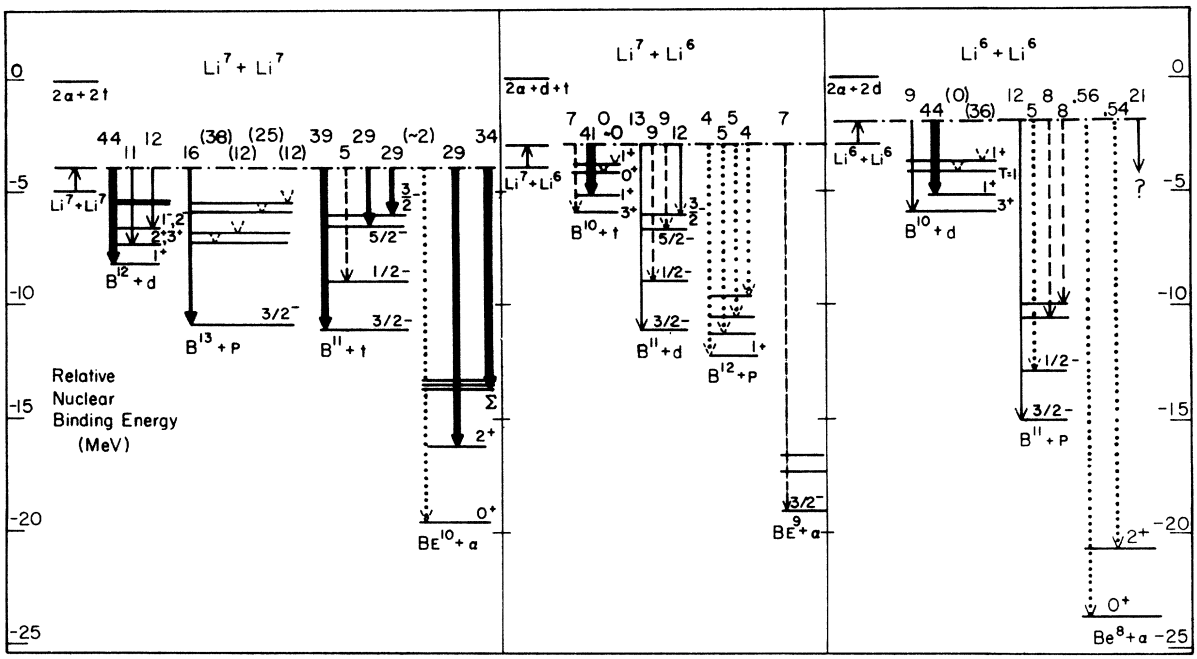

FIG. 13. Total cross sections for charged particle emission in Li-Li reactions at 2.1 MeV. Arrows represent kinetic energies and intensities of charged particles. Numbers above arrows are total cross sections$\times 10^{28}$ cm^2. J^π values apply to the residual nucleus. Numbers in parentheses are estimates from one point only (90°) in the angular distribution curve.

Be^9Li^7, where Allison[17] has pointed out that one only of the many possible exit channels, namely, that of $Be^9(Li^7,Li^8)Be^8$ has a cross section at 2 MeV, 17 times the calculated barrier penetration function for $l=0$ and 5 times the sum from $l=0$ to $l=3$. This would indicate that as targets, the nuclei Li^6 and Li^7 do not have the greatly extended structure which, in Be^9, includes the excursions of the unpaired neutron far from the electrical center of the nucleus.

We may also note that with these relatively heavy projectiles, the barrier penetration cross section may be greater for higher angular momenta ($l=1$) than for $l=0$. Thus we cannot *a priori* exclude the possibility of reaction through such higher angular momentum entrance channels, but in the absence of inhibiting factors about 1/3 of the total penetrations should be through the $l=0$ channels.

As to the relative values of the cross section for the production of certain groups, a few comparisons are possible between our results and the gamma-ray observations of Berkowitz *et al.*[2] Unfortunately, the gamma-ray studies cannot give relative populations of ground states, and our values of the first three excited states of B^{11} in $Li^7(Li^7,t)B^{11}$, $Li^7(Li^6,d)B^{11}$, and $Li^6(Li^6,p)B^{11}$ were used by them to calibrate their results. They made the slightly dangerous assumption that the relative level populations are only slightly affected by bombarding energy "at energies well below the Coulomb barrier," although their bombarding energies were approximately 4 MeV, carrying 2 MeV into the barycentric system, for a barrier height of 2.3 MeV. The assumption may be sufficiently precise if the kinetic energy of the ejected particle is large compared to the barrier height, but, for instance, in the case of the third excited state of B^{10} (2.15 MeV), we have not been able to see a triton group from it in the tritons from $Li^7(Li^6,t)B^{10*}$ ($Q=-0.162$

TABLE II. Cross sections for barrier penetration at 2-MeV accelerating voltage.

Target	projectile	Barrier[a] height B (MeV)	η cf. Eq. (4)	ϵ/B[b]	$\sigma_c=\pi\lambda^2(2l+1)T_l$ ($\times 10^{28}$ cm^2) $l=0$	$l=1$	$l=2$	$l=3$	$\sum_{l=0}^{3}\sigma_c$ ($\times 10^{28}$ cm^2)
Li^7	Li^7	2.2	5.3	0.45	55	80	12	8.4	155
Li^7	Li^6	2.3	4.5	0.43	76	108	38	5.5	228
Li^6	Li^6	2.4	4.9	0.42	142	203	56	1.7	403

[a] Calculated with nuclear radii given by $1.5A^{1/3}\times 10^{-13}$ cm.
[b] ϵ/B is (total translatory barycentric kinetic energy)/(barrier height).

[17] S. K. Allison, Phys. Rev. **119**, 1975 (1960). (The numerical value of Eq. 2 in this paper should be −1.54 MeV.)

MeV), whereas at higher bombarding energies Bromley *et al.*[18] have demonstrated the presence of tritons from this level at an intensity comparable to the strong group from the 0.72-MeV B^{10} level, and at 4 MeV Berkowitz finds the ratio of the population of this level to the population of the 0.72 level as 1.2/0.5.

In the case of the population of B^{10} levels from the $Li^6(Li^6,d)B^{10}$ reaction, we may compare our findings for the first three excited states (0.72, 1.74, and 2.15 MeV) with the gamma-ray results. The deuteron groups indicate population ratios corresponding to 44, 0, 36×10^{-28} cm^2, respectively; the gamma results give population ratios 4.4, <0.1, 6.0, which in view of the effect mentioned above in the discussion of $Li^7(Li^6,t)B^{10}$ seems fair agreement. There is apparently a lack of agreement in the population ratios in excited states of Be^{10} produced in $Li^7(Li^7,\alpha)B^{10}$. We find the 3.36-MeV and the sum of the 5.96-, 6.18-, and 6.26-MeV levels in the ratio 29 to 34×10^{-28} cm^2; the gamma-ray results are reported as ≥1.4 to 4.1. We cannot compare with the gamma-ray estimates of C^{13}, C^{12}, and C^{11} levels since these arise from neutron emission.

There is evidence from the relative values of the absolute cross sections portrayed in Fig. 13 that those reactions are favored in which a Li^7 can capture an alpha particle or a triton (if the other member of the reaction is a Li^7) or an alpha particle or a deuteron (if the other member is Li^6). The same may be said about the capture by Li^6 of an α or a triton from Li^7, or an α or a deuteron from another Li^6. Thus, the reactions producing protons do not stand out in importance, and are certainly minor in the Li^7Li^6 and Li^6Li^6 impacts. This suppression of protons occurs in spite of the enhancing effect of the relative ease of escape through the potential barrier. This is easy since the proton-producing reactions have high Q values and produce very fast protons, which have a low barrier height due to their single charge. In their gamma-ray studies of the population of levels of residual nuclei, Berkowitz *et al.*[6] have shown that the population of levels remaining after neutron emission is about equal to that from proton emission from the same reacting partners.

Li^6Li^6 Reactions

As illustrative of the suppression of proton emission in these reactions, we note that the deuteron exit channels in Li^6Li^6 involving the first and third (1^+) excited states of B^{10} exceed the total of four measured proton groups as 80 to 31, although the most energetic deuteron is about 4 MeV compared to the 13-MeV protons. Inclusion of the alpha channel would increase the ratio.

The lack of a deuteron group from the second excited (1.74 MeV, 0^+, $T=1$) state of B^{10} in $Li^6(Li^6,d)B^{10}$ has been discussed by Morrison.[2] Since then, the experimental fact of its absence has been verified by Bromley *et al.*[17] The effect may be explained as due to the operation of an isobaric spin selection rule, or to the impossibility of forming a 0^+ state of B^{10} by the addition of an α particle to Li^6 ($J=1^+$) in orbits of momenta $l=0$.

As we have seen, a very important exit channel from Li^6Li^6 is through the first excited state of B^{10} (0.72 MeV, 1^+, $T=0$). Here the necessary J value and parity are easily formed through the capture by Li^6 ($J^\pi=1^+$) of an α particle of no angular momentum relative to it; the alpha arising from the disruption of the other reaction member.

The α particles from Li^6Li^6 will be the subject of a later communication.

Li^7Li^6 Reactions

In the case of Li^7Li^6, the most probable exit channel we have measured is again through the 0.72-MeV 1^+ level of B^{10}, this time leaving a triton. The absence of a group from the 1.74-MeV $T=1$ level of B^{10} cannot be explained, as it was in the Li^6Li^6 reaction, by the isobaric spin conservation rule, it is, however consistent with the cluster reaction model (Morrison[2,3]). We do not have an explanation for the relatively low cross sections for B^{11} formation, which it would seem should be similar to the formation of the B^{10} 1^+ level in that this time the Li^7 captures the α particle instead of the deuteron from the disruption of the Li^6. Norbeck, however, has remarked that of two possible particle transfers, that which transfers the least mass is favored.

Li^7Li^7 Reactions

In the Li^7Li^7 reactions, the evidence is not so outstanding that the reacting clusters are undissociated Li^7 nuclei plus tritons and alpha particles. There is a strong exit channel involving the 1^+ ground state of B^{12} in which deuterons are emitted. For the proton channels we must to a considerable extent depend on cross sections somewhat precariously estimated under the assumption that the total cross section is approximately 4π times the barycentric differential cross section at 90°. Nevertheless, it seems unwarranted to assert that the protons are depressed with respect to other groups. The three groups of tritons from the ground, second, and third excited states of B^{11} are outstanding. These leave the B^{11} nucleus in a $3/2^-$ or $5/2^-$ state. The transition to the first excited B^{11} state ($J^\pi=1/2^-$, at 2.13-MeV excitation) is barely detectable. Such a state cannot be formed from a Li^7 by the capture of an alpha particle with $l=0$ with respect to it. The extreme weakness of the α group to the ground state of Be^{10} is noteworthy. Such a state, of $J^\pi=0^+$, cannot be formed by transfer of a triton to a Li^7 nucleus bringing in 0 units of orbital angular momentum.

[18] D. A. Bromley, K. Nagatani, L. C. Northcliffe, R. Ollerhead and A. R. Quinten, in *Proceedings of the Rutherford Jubilee International Conference, Manchester, England, 1961*, edited by J. B. Berks (Academic Press Inc., New York, 1961).

Angular Distributions

We may first make the general remark that unless polarizations are controlled, an angular distribution in the barycentric system is necessarily symmetric about 90° for the collision of identical nuclei. Thus, in some Li^7Li^7 reactions, data were not extended much beyond angles in the laboratory which transformed to 90° barycentric. Furthermore, as has previously been observed by Morrison,[8] angular distributions of, say Li^7Li^6 products can be extended to 180° in equipment mechanically limited to a lesser maximum angle, by interchanging target and projectile (Li^6Li^7), adjusting the bombarding energy and plotting $(\pi-\theta_c)$ instead of θ_c. Some of the Li^7Li^6 distributions have been extended in this manner.

Furthermore, it is certainly unsafe to attempt to interpret the angular distributions by comparing them with theoretical results which arise from an undistorted plane wave partial wave analysis. The value of η, which[19] is given by

$$\eta=(2Z_pZ_te^2/\hbar v_p)[T(T+P)/(T^2+P^2)], \qquad (4)$$

where Z_p, Z_t refer to the atomic numbers of projectile and target, respectively, P, T refer to the masses of the projectile and target, respectively, v_p is the initial velocity of the projectile in the laboratory system, is usually used as a criterion of the extent of the reliability of a description of elastic scattering based on hyperbolic inverse square law orbits. The classical orbital description becomes increasingly reliable as η exceeds unity, and from Table II we see that η is about 5, so a plane wave representation is inadequate.

In the following paragraphs we make some qualitative comments on the angular distributions. In these Li-Li collisions, it is not permitted to assume that only one initial partial wave (i.e., $l_1=0$) is involved since, as we have seen, T_l values are actually higher for $l_1=1$ than for $l_1=0$ and l_2 is quite appreciable. Furthermore, no resonances exist, enabling us to pick out a group of particles certainly associated with a well defined level in an intermediate nucleus.

Thus, in making some qualitative comments on the observed angular distributions, we will limit ourselves to only the most general principles, i.e., the conservation of angular momentum and parity. In some cases we can explain a close approach to angular isotropy or a wide departure from it, in a few, the observed facts seem contrary to expectation.

Some of the angular distributions shown in this paper have previously been given with relative ordinates and commented upon (Morrison[8]; Huberman and Morrison[1]). These are essentially the Li^7Li^6 reactions; they are shown here with absolute ordinates. New data, not previously offered, are as follows:

$Li^7(Li^7,p_0)B^{13}$; $Li^6(Li^6,p_0)B^{11}$, also p_1, p_2, p_3;
$Li^7(Li^7,d_0)B^{12}$, also d_1, d_2; $Li^6(Li^6,d_0)B^{10}$, also d_1;
$Li^7(Li^7,\alpha_1)Be^{10}$; $Li^6(Li^6,\alpha_0)Be^8$, also α_1, α_2.

$Li^7(Li^7,p)B^{13}$, $Li^7(Li^7,t)B^{11}$, and $Li^6(Li^6,p)B^{11}$

It is interesting to compare the angular distributions of particles from the above reactions, considering first those in which the residual boron isotope is left in its ground state. These are shown in Figs. 3, 5, and 11. It so happens that in the $l_1=0$ entrance channels, the operation of the Pauli principle makes the available J_1^π values 0^+ and 2^+ in both Li^7Li^7 and Li^6Li^6 encounters. If the shell-model assignment of $J^\pi=3/2^-$ to B^{13} is correct, all the residual nuclei have this same assignment. The intrinsic parities of proton and triton are positive. We might expect somewhat similar angular distributions, and this is the case for the protons from Li^7Li^7 and from Li^6Li^6, whose distributions are peaked at 90°. The tritons, however, from Li^7Li^7 are essentially isotropic.

The exit channels with $l_2=0$ cannot be excited through entrance channels with $l_1=0$, since the possible J_2^π values of the $l_2=0$ exit channels are 2^- and 1^-. Thus, it appears that the reaction proceeds through channels of higher l_1, which can excite exit channels with $l_2\geq 0$, thus, there is nothing surprising about the anisotropy of the protons.

We have seen that the yield of the tritons is remarkably large; to this may be added the different angular distribution as further evidence of the participation of the cluster reaction mechanism. Returning to the relative total cross sections for a moment, we see from Tables I and II that the ratio of the total cross section for these tritons to the sum of the barrier penetration cross sections for Li^7Li^7 from $l_1=1$ to $l_1=3$ is 0.39; for the Li^6Li^6 protons it is 0.042, less by a factor of 10. The Q value for the t_0 group is 6.21 MeV; large compared to the translational kinetic energy of 1 MeV in the barycentric system, and the linear momentum added to a triton after its associated α cluster has been captured is correspondingly large. Some fore and aft peaking, to be expected from a pickup reaction, added to the 90° peaking of the proton analogs would move in the direction of the observed triton isotropy.

The tritons (t_1) from Li^7Li^7 which leave B^{11} in its first excited state ($J^\pi=1/2^-$) show a markedly different angular distribution from that of the t_0 tritons, the change being consistent with the eight fold reduction in intensity and the fact that the simple alpha pickup mechanism cannot operate here. The distribution resembles, as it should, the p_1 distribution from $Li^6(Li^6,p_1)B^{11}$.

$Li^6(Li^6,d)B^{10}$ and $Li^7(Li^7,d)B^{12}$

The deuterons from the ground state ($J^\pi=3^+$) of B^{10} in $Li^6(Li^6,d_0)B^{10}$ show marked peaking at 90° and rela-

[19] In this form, η is the ratio of the classical perinuclear distance in a head-on collision to $(1/2\pi)$ times the de Broglie wavelength in the barycentric system.

tively low intensity (Figs. 12, 13). There are no special features of angular momentum and parity to explain these aspects, in fact a channel with $l_2=0$ and $J_2^\pi=2^+$ is available and matches the entrance channel $l_1=0$, $J_1^\pi=2^+$, thus allowing for a strong isotropic component. Under the reaction cluster mechanism, however, the α which is captured by Li^6 to form B^{10} must bring in two units of angular momentum, which requirement may favor an $l_1=2$ channel, capable of exciting anisotropy.

The deuteron groups from $Li^6(Li^6,d_1)B^{10*}$ and $Li^7(Li^7,d_0)B^{12}$ leave the residual nucleus in a 1^+ state. In the Li^6Li^6 case a simple pickup of an α cluster is possible. In the Li^7Li^7 case an α pickup is not possible, nevertheless the reaction cross section is large; we have previously remarked on this apparent contradiction to the cluster mechanism theory. The angular distribution of the Li^6Li^6 reaction (Fig. 12) is more nearly isotropic than is that from the Li^7Li^7 where the d_0's show a 90° maximum. We have previously noted in the $Li^6(Li^6,p_0)B^{11}$ reaction (α capture not possible) and the $Li^7(Li^7,t_0)B^{11}$ reaction (α capture possible) that the 90° peak of the former seems flattened out by the addition of the hypothetical fore and aft peaking of the latter. There may be a similar mechanism operating to make the Li^6Li^6 d_1's more isotropic than the d_0's from Li^7Li^7.

The absence of a detectable deuteron group in $Li^6(Li^6,d_2)B^{10*}$, in which B^{10*} has $T=1$, has previously been discussed.

$Li^7(Li^7,\alpha)Be^{10}$ and $Li^6(Li^6,\alpha)Be^8$

The low intensity of the alphas from the ground state of Be^{10} has previously been mentioned; due to it the angular distribution was not obtained. The angular distribution of the intense α group from Be^{10} in its first excited state (Fig. 6) shows fore and aft peaking but this cannot be used as pickup evidence, although simple triton capture is possible. An exit channel with $l_2=0$ and $J_2^\pi=2^+$ is open from the $l_1=0$, $J_1^\pi=2^+$ entrance channel. We were unable to resolve the alpha groups from the three Be^{10} levels near 6 MeV, some of which are certainly intense, hence angular distributions are not given.

The alpha particles from Li^6Li^6 present difficulties. The extreme weakness of the transition to the ground state of $Be^8(0^+)$ is not according to expectations; it could be produced by capture of a deuteron, and should be comparable in cross section to the simple α capture of $Li^6(Li^6,d_1)B^{10*}$. The extreme weakness of the ground-state transition has also been seen by Coste and Marquez.[20] Experiments on these alphas are in progress and will be the subject of a subsequent report.

Li^7Li^6 Reactions

The relative angular distributions for these reactions have been published and commented upon by Morrison. Since we are not dealing with identical projectiles and targets, 90° symmetry is not required in the barycentric system and indeed the angular distributions are mainly notable for their lack of symmetry about 90°. Thus, they do not proceed through a single state of definite J^π in a long-lived intermediate nucleus. One of the angular distributions departing farthest from fore and aft symmetry is that of the tritons in $Li^7(Li^6,t_1)B^{10}$, the B^{10} being left in its first excited 1^+ state ($T=0$). The Q value is relatively low, 1.27 MeV, and hence the momenta imparted to the reacting clusters through the action of nuclear forces is comparable with the translational momenta arising from the bombarding energy, and should not distort them in direction beyond all recognition. The tritons (cf. Fig. 9) are "emitted" mainly in the direction of motion of the Li^7 nucleus in the barycentric system, i.e., on the reaction cluster theory, they continue on in the original Li^7 direction after the alpha cluster of the Li^7 has been carried forward by the Li^6.

SUMMARY

The absolute cross sections and angular distributions of the charged particles emitted in the Li^7Li^7, Li^7Li^6, Li^6Li^6 nuclear reactions strongly suggest that a favored (but not necessarily the only) mechanism of reaction is by way of reacting clusters, consisting of the original nuclei and tritons, for Li^7, and deuterons for Li^6. If a new nucleus, in its ground or in an excited state, can be formed with the correct J by the welding together of one of the original nuclei and a reacting cluster, with zero angular momentum between them, this will be an outstanding mode of interaction. Prominent examples in the Li^7Li^7 reactions are the capture of an α cluster to form states of B^{11} of $3/2^-$, and of a triton to form Be^{10} in its 2^+ excited state. The capture of an α cluster by Li^6 to form B^{10} in its 1^+ excited state is highly probable. An apparent exception, difficult to reconcile with the above simplicity, is the prominent emission of deuterons in the Li^7Li^7 interactions.

The reacting cluster picture begs the question of whether a cluster model is appropriate to an isolated Li^6 or Li^7 nucleus. It is quite permissible to state that the clusters only become prominent in the distortions caused by the intense forces acting during the encounter. The analogy of the Butler stripping mechanism to the capture of an α cluster by a passing Li nucleus is not very close. The diffraction pattern zeros of the typical Butler[21] analysis, as has been shown in a classical interpretation of it, require a length, i.e., the nuclear diameter of the target, and the assumption that the light projectile (usually a deuteron) is stripped on the nuclear surface, with coherent interference of the waves from opposite surface areas. With the reacting clusters of the present case, where the mass of the cluster is at

[20] M. Coste and L. Marquez, Compt. Rend. **254**, 1768 (1962).

[21] S. T. Butler, N. Austern, and C. Pearson, Phys. Rev. **112**, 1227 (1958).

least 2/7 that of any nucleus present, a reaction diameter is difficult to imagine. Thus, the typical Butler diffraction patterns are probably not well defined in the angular distribution of the continuing fragment even at higher bombarding energies where plane waves are more nearly applicable. Much more work with various bombarding energies is needed to fill out these tentative suggestions or to discard them for a better understanding of the reaction mechanisms.

A cluster interpretation of nuclear transformations involving lithium projectiles has been previously suggested by Bashkin,[22] although in somewhat more detail than ours.

ACKNOWLEDGMENTS

This work was part of a program of research under the sponsorship of Professor S. K. Allison. We are indebted to him for aid in the preparation of this paper. We wish to thank Larry Palmer and John Erwood for operation and maintenance of the Van de Graaff accelerator and the electronic equipment.

[22] S. Bashkin, University of Iowa Report SUI-61-6 (unpublished).

PHYSICAL REVIEW VOLUME 129, NUMBER 2 15 JANUARY 1963

Nuclear Reactions Induced by the Nitrogen Bombardment of Boron-11, Fluorine, Aluminum, Silicon, Phosphorus, and Chlorine

E. NEWMAN AND K. S. TOTH
*Oak Ridge National Laboratory, Oak Ridge, Tennessee**

(Received 24 August 1962)

Cross sections as a function of bombarding energy were obtained from thick target yields for twelve reactions induced by 27.5-MeV nitrogen ions accelerated in the ONRL 63-in. Cyclotron. Materials containing the following six elements were bombarded: boron, fluorine, aluminum, silicon, phosphorus, and chlorine. The irradiated materials were γ counted and the radioactive products were identified by their characteristic γ rays and half-lives. The following nuclides were observed: Ne^{23} from B^{11}; P^{30} from F^{19}; K^{38} from Al^{27}; Cl^{34m} and K^{38} from silicon; Sc^{43} from P^{31}; Sc^{43}, Sc^{44}, Sc^{44m}, Ti^{45}, and V^{47} from Cl^{35}; and Cr^{49} from Cl^{37}. The observed cross sections are in general agreement with those obtained from other heavy-ion induced reactions at these energies. For the target nucleus Cl^{35} it was possible to identify five products, and experimental cross-section ratios were compared to the theoretical ratios determined from Monte Carlo evaporation calculations.

INTRODUCTION

ONE of the many reaction mechanisms available for study with incident heavy ions is the formation and subsequent decay of a compound system via the evaporation of light particles. Heavy ions are particularly useful in producing a compound system because of the large excitations available at relatively low bombarding velocities. It has been found from previous experiments with N^{14} ions at these energies that, with the exception of transfer reactions, direct interactions are essentially negligible.[1] The predictions of the statistical theory of compound nucleus decay should, therefore, be directly applicable to the distribution of final nuclei after the decay of the compound system.

Several workers have previously determined total cross sections for compound nucleus reactions induced by 27.5-MeV N^{14} ions. Targets which have been studied include carbon,[2] beryllium,[3] boron and oxygen,[4] aluminum,[5] sodium,[6] potassium,[7] and sulfur.[8] In the present work, total cross sections were determined as a function of bombarding energy for twelve reactions leading to radioactive end products. In all, six different target materials were bombarded. Information concerning these reactions is summarized in Table I. The observed final products can be made by various combinations of emitted particles starting with a given compound nucleus. The assumed decay mode for a particular end-product is also listed in the table. The investigated reactions supplement the previous measurements and provide a more complete picture for reactions initiated by the nitrogen bombardment of elements ranging from lithium to potassium.

EXPERIMENTAL METHOD

The following materials were irradiated in the 27.5-MeV N^{14} deflected beam of the ORNL 63-in. Cyclotron:

* Operated for the U. S. Atomic Energy Commission by the Union Carbide Corporation.

[1] A. Zucker, Ann. Rev. **10**, 27 (1960).
[2] H. L. Reynolds and A. Zucker, Phys. Rev. **96**, 1615 (1954).
[3] H. L. Reynolds and A. Zucker, Phys. Rev. **100**, 226 (1955).
[4] H. L. Reynolds and A. Zucker, Phys. Rev. **102**, 237 (1956).
[5] W. H. Webb, H. L. Reynolds, and A. Zucker, Phys. Rev. **102**, 749 (1956).
[6] M. L. Halbert, T. H. Handley, and A. Zucker, Phys. Rev. **104**, 115 (1956).
[7] J. J. Pinajian and M. L. Halbert, Phys. Rev. **113**, 589 (1959).
[8] D. E. Fisher, A. Zucker, and A. Gropp, Phys. Rev. **113**, 542 (1959).